

Dielectric Relaxation in $\text{Cd}_x\text{InSe}_{9-x}$ Chalcogenide Thin Films

A. Abdel Aal

Physics Department, Faculty of Science, Helwan University, Egypt.

The effect of temperature (273-493 K), frequency (10^2 - 10^5 Hz) and composition on the dielectric response of the $\text{Cd}_x\text{InSe}_{9-x}$ ($x= 1,2,3,4$ and 5) Chalcogenide glass system was studied. The experimental results indicate that dielectric constant (real permittivity), dielectric loss and loss angle ϵ' , ϵ'' and $\tan \delta$, increase with increasing temperature. The complex impedance (Z) was measured over the same temperature and frequency ranges. All samples gave a semicircle arc originating at the origin point. This indicates that each composition can be described only by one bulk resistance R_b and one capacity C_b , both parallels combined. The centre below the real axis indicates the relaxation behaviour of the system. The dielectric dispersion is characterized by the distribution of the relaxation time induced by polarized species contribution (orientational, interfacial, electronic and ionic dipoles). The free energy (ΔF) and the enthalpy (ΔH) of the dipoles are estimated for the investigated compositions.

1. Introduction:

Chalcogenide glasses have attracted researchers' interest because of their potential use in opto electronic and technological applications such as photo resists, image storage, and memory switching. AC conductivity and dielectric measurements have been reported for a wide variety of amorphous Chalcogenide semiconductors [1-7] in order to understand the mechanisms of conduction processes in these materials and the types of polarization. Chalcogenide glasses with low phonon energies and high refractive indices were found to be efficient host materials for fiber-optics amplifiers and infrared lasers when doped with rare earth ion [8]. Further, chalcogenides found wide applications in the field of information storage and power control devices, etc... [9, 10]. The aim of the present work is to investigate the dielectric characteristics of the multi components Chalcogenide system $\text{Cd}_x\text{InSe}_{9-x}$.

2. Experimental Techniques:

The amorphous Chalcogenide compositions of Cd_xInSe_{9-x} were synthesized from 5N purity elements in evacuated sealed silica ampoules heated for 12 h at 1000 °C in rotating furnace and then quenched in 0 °C. Thin films of the Cd_xInSe_{9-x} were obtained by conventional thermal evaporation technique of the investigated composition on to cleaned glass substrates using high vacuum coating unit (Edwards type E 306A), and at 10^{-6} Torr. The deposition rate (4-6 nm/sec) and film thickness were controlled with the quartz crystal thickness monitor and also confirmed optically by multiple beam interferometer. The X-ray patterns for all thin films show no peaks confirming the disordered state.

Chemical composition of thin films was checked by energy dispersive X-ray analysis (EDX) on Joel 6400 scanning electron microscope. Fig (1) shows, as an example, the EDX pattern for the thin film of composition Cd_3InSe_6 . Table (1) contains the atomic percentage for various Cd_xInSe_{9-x} thin films. The electrical measurements were carried out on sandwiched structure formed between two thick metal gold electrodes of typical thickness deposited prior and after deposition of $Cd_x InSe_{9-x}$ films using thermal evaporation technique. The ohmic behaviour of contacts has been checked before the measurements. The films thickness is 0.3 μm and the effective area is $4.0 \times 10^{-6} \text{ m}^2$. A programmable automatic RCL bridge (PM 6304 Philips with operating frequency range 50 Hz – 100 kHz) was used to measure the Capacitance C , Impedance Z , and the phase angle Φ between voltage and current on the sample, ac voltage of the test signal is normally 1v, and dc bias is off. Ni/Cr thermocouple was used for measuring the temperature with the help of an automatic digital temperature controller.

The dielectric constant ϵ' (real part) was calculated using the relation:

$$\epsilon' = Cd/\epsilon_0 A \quad (1)$$

where C is the capacitance of the film, A is the cross sectional area of the parallel surfaces of the samples, d is the film thickness (0.3 μm) and ϵ_0 is the permittivity of the free space. The imaginary part of the dielectric constant ϵ'' was calculated using the relation:

$$\epsilon'' = \epsilon' \tan\delta \quad (2)$$

where: $\tan\delta = \tan(90-\phi)$. (3)

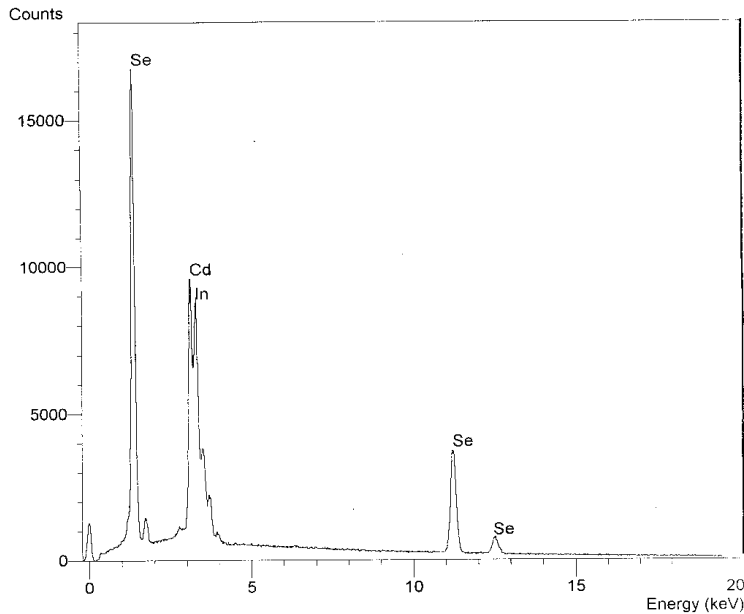


Fig. (1): EDX analysis for $\text{Cd}_3\text{In}_1\text{Se}_6$ thin film.

Table (1): Energy Dispersive X-Ray (EXD) spectroscopy for thin film of $\text{Cd}_x\text{InSe}_{9-x}$.

x	Cd (at %)	In (at %)	Se (at%)
1	8.967	11.023	80.015
2	23.548	10.067	66.382
3	35.868	10.730	53.420
4	36.147	12.188	51.662
5	46.270	9.620	44.122

3. Results and Discussion:

3.1. Frequency and Temperature dependence:

Figure (2). represents the frequency dependence of the real permittivity ϵ' of thin film of the Cd_3InSe_6 composition at different temperatures. As shown in the figure, ϵ' decreases with the increase of frequency and approaches a flat value at higher frequencies, and increases with the increasing temperature. The other compositions of the system $\text{Cd}_x\text{InSe}_{9-x}$ have the same trend with the frequency and temperature. It is clear that the above mentioned results are not in accordance with those of the Debye's type characterized by a single relaxation time. Hence, in the $\text{Cd}_x\text{InSe}_{9-x}$ system there is a possible distribution of

relaxation times. In addition to having usual defects such as cracks and microvoids, amorphous compounds have local imperfections such as distorted bond angles and defect centers, either of which can, at sufficiently high concentration yield localized states in the gap known as dangling bonds, which can have three charge states as D^+ , D^- and D^0 . These defects are responsible not only for the position of the Fermi energy, but also for the transport properties of the materials. In addition, they act as traps and recombination centers for carriers and D^+/D^- centers in close proximity forming a dipole possibly responsible for dielectric behaviour. When the sample is placed in an electric field, the electrons hop between localized sites. The charge carriers moving between these sites hop from a donor to an acceptor state. Consequently, each pair of sites forms a dipole and contributes to dielectric relaxation.

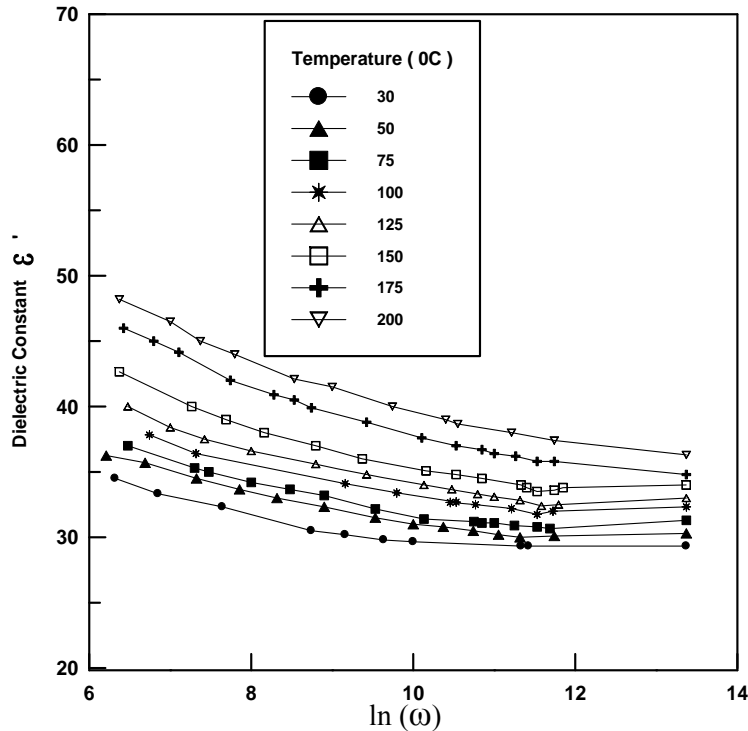


Fig. (2): Variation of dielectric constant ϵ' with $\ln(\omega)$ for Cd_3InSe_6 at different temperatures.

In Chalcogenide glasses, the dielectric properties can be interpreted by considering a set of dipoles as long as the temperature is high enough. Each dipole has a relaxation time depending on its activation energy which is attributed to the existence of a potential barrier W over which the carriers must

hop. The total polarization in any dielectric material is made up of four different components according to the nature of the displaced charge. The average dipole moment per molecule is given by [11]:

$$\mu = \alpha_p E,$$

and the electric polarization by,

$$P = N \alpha_p E, \quad (3)$$

where N is the number of molecules per unit volume, E is the electric field intensity acting on each molecule, and α_p is the total polarizability,

$$\alpha_p = \alpha_e + \alpha_i + \alpha_o + \alpha_s \quad (4)$$

where α_e , α_i , α_o and α_s are the electronic, ionic, orientational, and interfacial or space charge polarizabilities.

Increasing the frequency of the applied field tends to decrease the orientational polarization, since it takes more time than the electronic and ionic polarization. This leads to a decrease of the dielectric constant with the increase of frequency. The real permittivity ϵ' increases with the increase of temperature T , and this behaviour can be attributed to the fact that orientational polarization is associated with the thermal motion of molecules. The orientation of the molecules of dipoles increases as the thermal energy increases, leading to the increase of the dielectric permittivity.

Figure (3) represents $\log \epsilon''$ vs $\log \omega$ for Cd_3InSe_6 at different temperatures (the other compositions have the same trend). As the temperature increases, the dielectric loss ϵ'' increases, especially at low frequency. This may be due to the increase in the conduction with T , so the conduction losses increase also and an exponential decay occurs with $\log(\omega)$. No indication of a maximum peak is observed in the dielectric loss ϵ'' in the region of frequency dependence. It is revealed that for Chalcogenide glasses [12-14]:

$$\epsilon'' = A \omega^m \quad (5)$$

The experimental values of the power m are equal to $-4\pi kT / W_m$, W_m can be considered as the work done in polarizing the dielectric.

When an electric field acts on any dielectric, the latter dissipates a certain quantity of electric energy that transforms into heat energy. This phenomenon is known as power loss, and the amount of power loss is commonly known as dielectric loss. This loss is a function of frequency and temperature and is related to relaxation polarization, in which the dipole cannot follow the field variation without a measurable lag because of the retarding or friction forces of the rotating dipoles.

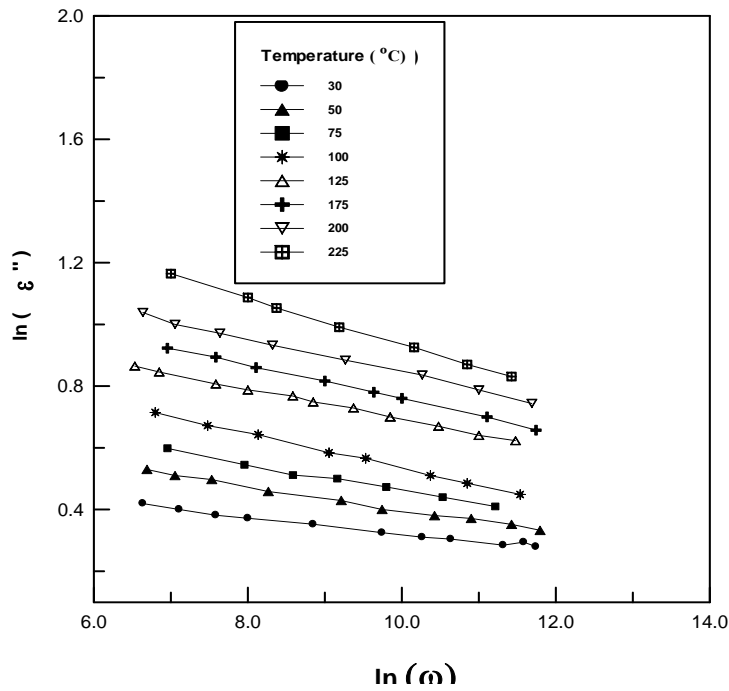


Fig. (3): Variation of dielectric loss, $\ln \varepsilon''$ with $\ln(\omega)$ for Cd_3InSe_6 at different temperatures.

Also, when the polarization of the dielectric changes, a polarizing current flowing in the dielectric is induced by the relaxation rate, this current induces dielectric loss in the material. In turn, the activation energy and the entropy for dielectric originate due to dipole rotation or movement of molecules during the relaxation process under the applied field. The calculated values of W_m for the different x values and the different temperatures are given in Table (2), it is clear that the activation energy W_m at 303K increases firstly from 0.37eV for Cd_1 to 1.54 eV for Cd_2 . This may be attributed to the change of conduction from localized states near the Fermi level to the extended states, indicating that hopping is dominant in Cd_1 and free bands in Cd_2 . As the Cd concentration increases, the activation energy decreases from 1.54 eV for Cd_2 to 0.75 eV for Cd_5 . This behavior is due to the creation of more charge carriers and the decrease of the charged centers in the gap. It also may be due to the replacement of Se-Se bonds of strength with $(332 \pm 0.4 \text{ KJmol}^{-1})$ with Cd-Se bonds of strength $(127.6 \pm 25.1 \text{ KJmol}^{-1})$

Table (2): The power factor m and the activation energy W_m .

Composition	Temperature (K)	m	W_m (eV)
Cd ₁	303	-0.28	0.37
	323	-0.32	0.36
	348	-0.34	0.35
	373	-0.38	0.34
	398	-0.43	0.32
	423	-0.46	0.32
	448	-0.50	0.31
Cd ₂	303	-0.07	1.54
	323	-0.09	1.19
	348	-0.12	1.01
	373	-0.26	0.89
	398	-0.32	0.85
	423	-0.36	0.80
	448	-0.36	0.78
Cd ₃	303	-0.10	1.06
	323	-0.12	0.90
	348	-0.15	0.81
	373	-0.16	0.79
	398	-0.18	0.76
	423	-0.19	0.74
	448	-0.20	0.63
Cd ₄	303	-0.08	0.86
	323	-0.16	0.73
	348	-0.18	0.66
	373	-0.23	0.55
	398	-0.27	0.52
	423	-0.29	0.50
	448	-0.33	0.48
Cd ₅	303	-0.14	0.75
	323	-0.15	0.71
	348	-0.16	0.63
	373	-0.20	0.51
	398	-0.36	0.38
	423	-0.39	0.37
	448	-0.43	0.36

The variation of the loss factor ($\tan \delta$) with temperature for Cd_3InSe_6 at different frequencies is shown in Fig.(4). It is clear that ($\tan \delta$) increases with the increase of temperature at all frequencies. The variation is most prominent at lower frequencies. The decrease of ($\tan \delta$) with frequency is more rapid at high temperatures; this may be attributed to interfacial polarization in that region. The charge carriers existing in the dielectric film can migrate for some distance under the influence of an applied electric field. When such carriers are blocked at the electrodes, a space charge region results. This leads to a substantial increase in ($\tan \delta$) towards low frequencies [15].

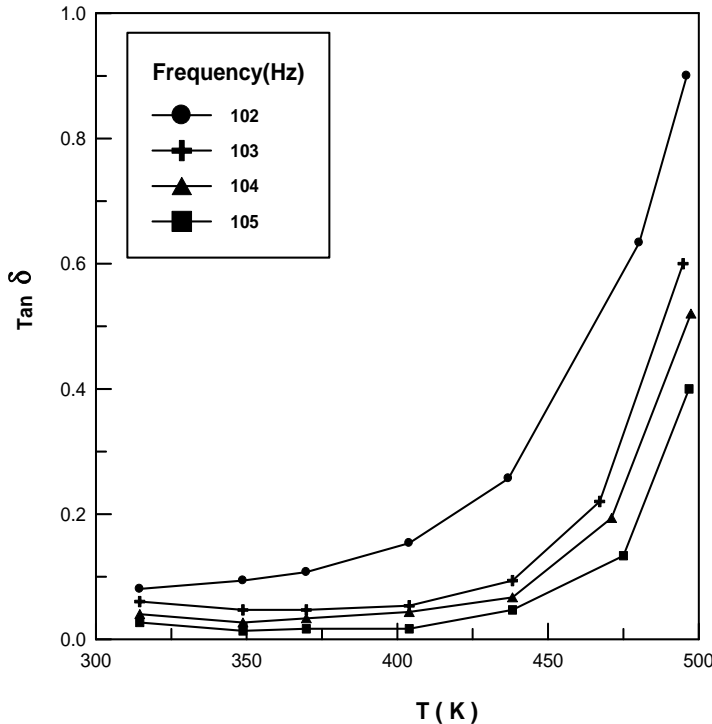


Fig. (4): Variation of loss angle $\tan \delta$ with T for Cd_3InSe_6 at different constant frequencies.

3.2. Distribution parameter (α) and relaxation time (τ):

The behaviour of most dielectric materials departs in varying degrees from the Debye response. The Cole-Cole expression is given by [16, 17]:

$$\varepsilon(\omega) - \varepsilon(\infty) \sim 1 / (1 + i\omega\tau)^{1-\alpha} \tag{6}$$

where $\varepsilon(\omega)$ is the complex permittivity, $\varepsilon(\infty)$ represents the free space or the permittivity at a sufficiently high frequency where the losses are negligible, α is

the parameter denoting the angle of tilt of the circular arc from the real axis, and τ is the relaxation time.

The Cole –Cole curves are also useful to confirm the distribution of the relaxation time. Fig.(5). shows the typical Cole-Cole curves at different temperatures for Cd_3InSe_6 as an example. The representations are an arc of a circle intersecting the abscissa axis at the values ϵ_∞ and ϵ_s and having its center lying below the real axis. ϵ_∞ and ϵ_s are the optical and static dielectric constants. The radius is drawn through the center and ϵ_∞ makes an angle $\alpha\pi/2$ with the real axis. $\tan \alpha\pi/2$ is determined from the plots, α is calculated ($0 < \alpha < 1$), and τ_0 can be determined from the relation:

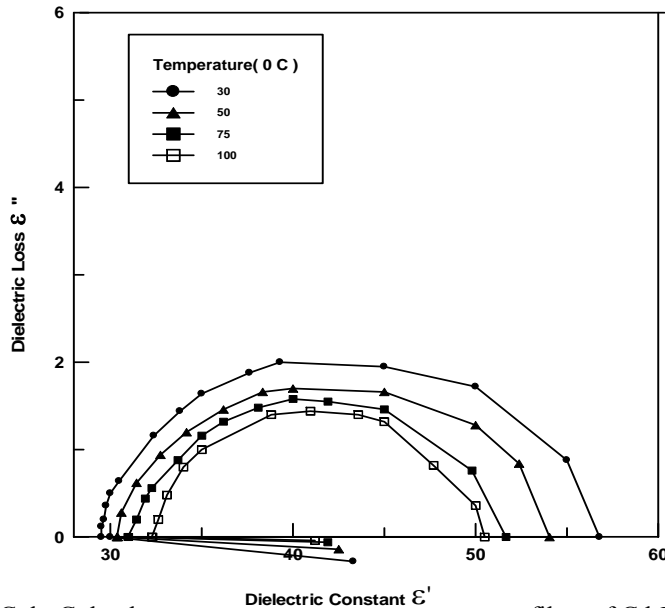


Fig. (5): Cole-Cole plots at different temperatures for thin films of Cd_3InSe_6 .

$$V/u = (\omega\tau_0)^{(1-\alpha)} \tag{7}$$

where V is the distance on the Cole-Cole curves between ϵ_s and the experimental point, u is the distance between the experimental point and ϵ_∞ , ω is the angular frequency, and τ_0 is the macroscopic relaxation time.

The molecular relaxation time τ can be estimated from the values of τ_0 at different temperatures for every value of x from the relation [18]:

$$\tau = [(2 \epsilon_s + \epsilon_\infty) / 3\epsilon_s] \tau_0 \tag{8}$$

The determined values of τ , ϵ_s , ϵ_∞ and τ_0 are indicated in Table (3), it is clear that as the Cd content increases, the static permittivity increases. This is attributed to the increase of $Cd^+ - Se^-$ dipoles concentration in the amorphous

matrix. The dependence of dielectric constant on the Cd content can be interpreted as a compositional disorder change.

From Table (3) and with the concept of molecular relaxation, it is clear that for every composition alone static permittivity ϵ_s increases with T, because the increase in thermal energy will break the intermolecular interaction, resulting in reduction of the values of macroscopic relaxation time τ .

Table (3): Cole-Cole representation parameters.

Composi- tion	T (K)	τ_0 (sec)	ϵ_s	ϵ_∞	T (sec)	Free energy ΔF (kcal mole ⁻¹)	Enthalpy ΔH (kcal mole ⁻¹)
Cd ₁	303	9.0x10 ⁻⁴	36.4	25.5	8.1x10 ⁻⁴	13.5	14.72
	323	5.6x10 ⁻⁵	35.6	26.2	5.1x10 ⁻⁵	12.9	
	348	2.2x10 ⁻⁵	34.0	26.5	2.1x10 ⁻⁵	13.0	
	373	9.3x10 ⁻⁵	32.6	27.2	8.8x10 ⁻⁶	13.4	
Cd ₂	303	1.9x10 ⁻⁴	40.9	35.3	1.9x10 ⁻⁴	12.6	16.56
	323	9.0x10 ⁻⁵	40.2	35.6	8.7x10 ⁻⁵	12.9	
	348	5.1x10 ⁻⁵	39.8	35.8	4.9x10 ⁻⁵	13.6	
	373	3.9x10 ⁻⁵	38.8	36.5	3.8x10 ⁻⁵	14.5	
Cd ₃	303	2.1x10 ⁻⁴	56.9	29.3	1.8x10 ⁻⁴	12.6	17.48
	323	4.7x10 ⁻⁵	51.1	30.2	4.1x10 ⁻⁵	12.5	
	348	3.4x10 ⁻⁵	51.7	30.9	2.9x10 ⁻⁵	13.1	
	373	1.7x10 ⁻⁵	50.2	32.1	1.5x10 ⁻⁵	15.2	
Cd ₄	303	6.3x10 ⁻⁴	56.9	29.3	1.8x10 ⁻⁴	13.0	16.1
	323	5.2x10 ⁻⁵	51.1	30.2	4.1x10 ⁻⁵	13.8	
	348	4.2x10 ⁻⁵	51.7	30.9	2.9x10 ⁻⁵	13.5	
	373	1.5x10 ⁻⁵	50.2	32.1	1.5x10 ⁻⁵	13.7	
Cd ₅	303	3.7x10 ⁻⁴	58.8	31.8	3.1x10 ⁻⁴	12.9	15.64
	323	4.1x10 ⁻⁵	53.6	33	3.6x10 ⁻⁵	12.4	
	348	3.0x10 ⁻⁵	51.0	34	2.7x10 ⁻⁵	13.0	
	373	1.9x10 ⁻⁵	48.8	36.4	1.7x10 ⁻⁵	13.9	

3.3. Impedance of $\text{Cd}_x\text{InSe}_{9-x}$ system:

When the dielectric is polarized, the dipoles may execute consecutive hops between sites arranged in three dimensional arrays, such hopping charges can contribute to dc conductivity as well as giving a finite ac effect. The natural form of representation is the impedance diagram. Here the bulk region dielectric is characterized by parallel bulk dc conductance G_b or bulk resistance R_b , and bulk capacitance C_b corresponding to the physical dimension of the entire sample and this is related to relaxation time $\tau (=C_b / G_b)$. Hence, impedance analysis is required to determine an appropriate equivalent circuit for the prepared samples. The plots of Z' vs Z'' (Z' is the real part of impedance and Z'' is the imaginary part) for Cd_3InSe_6 were recorded at different temperatures over the frequency range 10^2 - 10^5 Hz, (Fig. 6). Semicircular arcs were obtained, originating at the origin point with their centers lying below the real axis and cutting this axis at the origin and at $Z'=1/G$, where G is the conductance. Since the impedance plot gives only one semicircle originating at (0,0), this indicates that the composition can be represented by two physical different regions which are in parallel with one another with the same reference voltage, a bulk resistance R_b in parallel with a capacitor C_b . The values of the real and imaginary components for such circuits are given by:

$$Z' = R / (1 + \omega^2 C^2 R^2) = Z \cos \Phi \quad (9)$$

$$Z'' = \omega CR^2 / (1 + \omega^2 C^2 R^2) = Z \sin \Phi \quad (10)$$

where Φ is the phase angle between the current and the voltage on the sample.

3.4 Thermodynamic parameters:

From Eyring theory [19] the relaxation time is related to the free energy by the following expression [20, 21]:

$$\tau = (h/kT) \exp(\Delta F/RT) \quad (11)$$

where ΔF is the Gibbs free energy of activation for dipole relaxation during rotation, R is the gas constant, k is Boltzmann's constant and h is Planck's constant. Since, $H = U + PV$, where H is the enthalpy, P is the pressure and V is the volume, U is the internal energy and it is a function of temperature and is equal to the sum of kinetic and potential energy of the components particles of the system ($dU = TdS - PdV$). Then due to the rotation of the dipoles, and their resistance against the forces of friction in the viscous medium and some time the transition of ions from one site to another, this leads to changing of potential energy of the species and so they need to be activated (W_m), resulting in a

change of internal energy and entropy of the system. Then, H is a function of T . Further, ΔF is related to the enthalpy of activation ΔH and entropy of activation ΔS by the relation:

$$\Delta F = \Delta H - T\Delta S \tag{12}$$

According to Eqn. (11) and (12), the plot of $\log(\tau.T)$ vs $1/T$ (Fig.7) gives a linear relation with slope equal to $\Delta H/R$ from which ΔH can be calculated. Table (3) contains the calculated values of ΔF and ΔH .

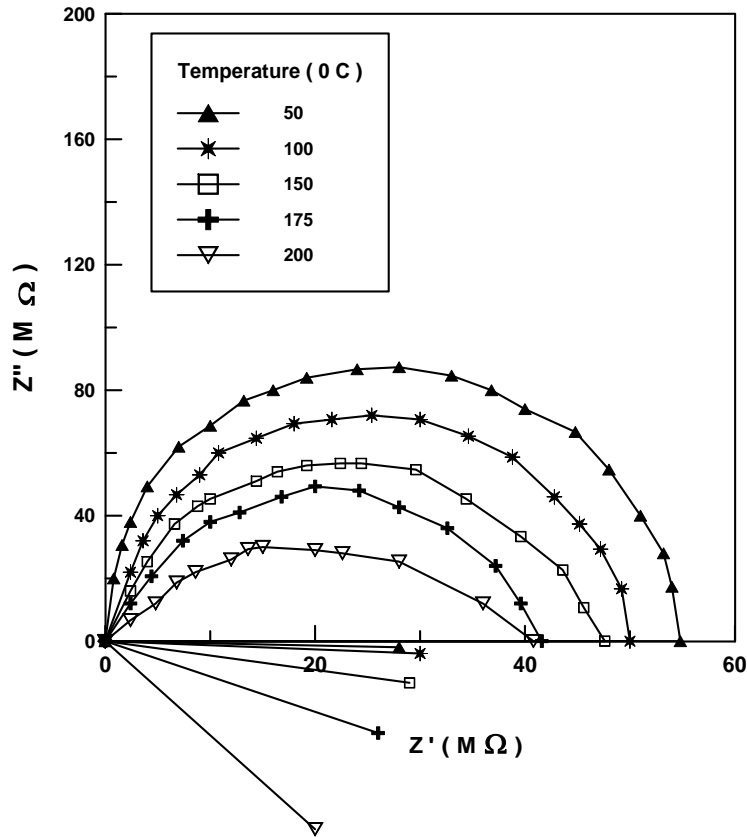


Fig. (6): Impedance plots Z' , Z'' at different temperatures for thin films of $Cd_3In_1Se_6$.

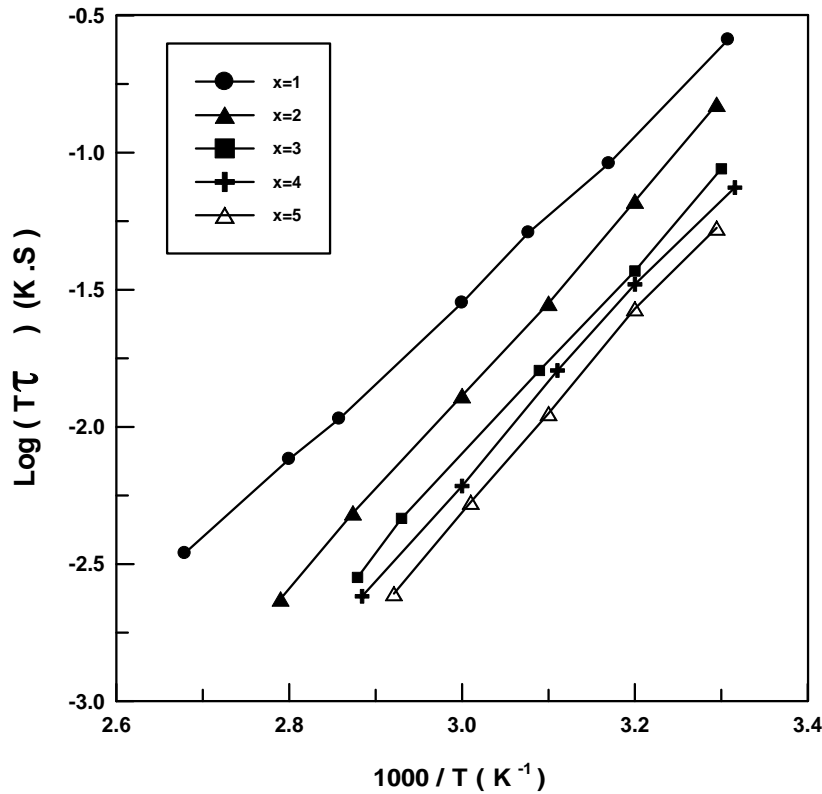


Fig. (7): Variation of relaxation time with temperature for the Cd_xInSe_{9-x} system., for various x values.

Conclusion:

- Thin films of $Cd_xInSe_{(9-x)}$ system of thickness 0.3 μm were prepared by the thermal evaporation technique. Dielectric constant ϵ' and dielectric loss ϵ'' are frequency and temperature dependent.
- The curves of the dielectric relaxation revealed a behavior different from Debye's type with a single relaxation. For $Cd_xInSe_{(9-x)}$ chalcogenide system a relaxation distribution was caused by a combination of polarized charge particles, such as interfacial and orientational polarization and other charges.
- AC measurements at various values of T and ω were used to design the equivalent circuits for all compositions. All samples could be represented by resistance R_b connected in parallel with a capacitance C_b .
- Enthalpy energy ΔH and the free energy ΔF for the dipoles rotation and the movement of polar molecules were obtained.

References:

1. N. M. Megahid, *Chinese Journal of Physics*, **41**(2), 130 (2003).
2. F. Salman, *Turk J. Phys*, **28**, 41 (2004).
3. M. M.El-Samanoudy, *J. Phys: Condens. Matter*,**14**, 1199 (2002).
4. A. Abdel-Aal, *J. Mater. Sci. Technol*, **14**, 247 (1998).
5. R. A.Bitar and D. E. Arafah, *Sol. Energy Mater Sol. Cells* **51**, 83 (1998).
6. A .E .Owen: *Glass Ind.*, **48**, 637(1967).
7. K. Sedeek, A. Adam, L. A. Wahab and F. M. Hafez., *Materials Chemistry and Physics* **85**, 20 (2004).
8. K. Abe, H.Takebe, and K.Morinaga, *J. Non-Crys. Solids*, **212**, 143(1997).
9. M.A.Redwan, E.H.Aly, L.I.Soliman, A.A.El-Shazely and H.A. Zayed., *Vacuum* **69**(4), 545(2003).
10. M .A. M. Seyam., *Applied Surface Science*, **181**, 128(2001).
11. B. Tareev, “*Physics of Dielectric Materials*”, Mir Publisher Moscow, (1979).
12. J. C. Giuntini, J. V. Zanchetta, D. Jullien, R. Eholie and P.Houenou: *J. Non- Cryst. Solids*, **45**, 57 (1981).
13. N.F.Mott, E.A. Davis and R. A. Street. *Phil. Mag.* **32**, 961 (1975).
14. R. A. Street and N. F. Mott, *Phys. Rev. Lett.* **35**, 1293 (1975).
15. A.VON Hippel, E.P.Gross, F.G. Telstis, and A. Geller, *Phys. Rev.* **91**, 568 (1953).
16. K. Jonscher, *Dielectric relaxation in solids (Chelsea Dielectrics Press London 1983)*.
17. R. H. Cole and K. S .Cole: *J. Chem. Phys*, **9**, 341(1941).
18. J. G. Powles, *J. Chem. Phys.* **21**, 633(1953).
19. H. Eyring, *J. Chem. Phys.* **4**, 283 (1936).
20. A.E.Stearn and H. Eyring, *J. Chem. Phys.* **5**, 113 (1937).
21. S.Glasstone, K. J. Laidler and H Eyring, “*The Theory of Rate Processes* (Mc Graw-Hill, New York, 1941) P.544.